View metadata, citation and similar papers at core.ac.uk

brought to you by CORE

New Journal of Physics
The open access journal at the forefront of physics

Deutsche Physikalische Gesellschaft DPG IOP Institute of Physics

PAPER • OPEN ACCESS

Observation of photon-pair generation in the normal group-velocity-dispersion regime with slight detuning from the pump wavelength

To cite this article: Kyungdeuk Park *et al* 2018 *New J. Phys.* **20** 103004

View the article online for updates and enhancements.

IOP ebooks™

Bringing you innovative digital publishing with leading voices to create your essential collection of books in STEM research.

Start exploring the collection - download the first chapter of every title for free.

This content was downloaded from IP address 141.223.153.36 on 04/06/2019 at 02:38

New Journal of Physics
The open access journal at the forefront of physics

Deutsche Physikalische Gesellschaft DPG
IOP Institute of Physics

Published in partnership with: Deutsche Physikalische Gesellschaft and the Institute of Physics

OPEN ACCESS

RECEIVED
6 June 2018

REVISED
10 September 2018

ACCEPTED FOR PUBLICATION
14 September 2018

PUBLISHED
5 October 2018

Original content from this work may be used under the terms of the Creative Commons Attribution 3.0 licence.

Any further distribution of this work must maintain attribution to the author(s) and the title of the work, journal citation and DOI.

PAPER

Observation of photon-pair generation in the normal group-velocity-dispersion regime with slight detuning from the pump wavelength

Kyungdeuk Park, Dongjin Lee, Yong Sup Ihn, Yoon-Ho Kim and Heedeuk Shin

Department of Physics, Pohang University of Science and Technology (POSTECH), Pohang 37673, Republic of Korea

E-mail: heedeukshin@postech.ac.kr

Keywords: photon-pair generation, spontaneous four-wave mixing, phase matching condition, normal group-velocity dispersion

Abstract

A fiber-based photon-pair source in the telecom C-band is suitable for quantum information science including quantum communications. Spontaneous four-wave mixing effects are known to create photon pairs that are slightly detuned from the pump wavelength only in the anomalous group-velocity-dispersion (GVD) regime. Here, we achieve high-quality photon-pair generation slightly detuned from the pump wavelength in the normal GVD regime through a dispersion shifted fiber, for the first time. The photon pairs in C-band exhibit strong temporal correlation with each other and excellent heralded anti-bunching property. This photon-pair generation scheme can be exploited as telecom-band quantum light sources for quantum information applications.

A non-classical light source is one of the key elements of quantum information processing systems, and several types of these sources have been investigated, including molecules [1], trapped atoms [2], quantum dots [3], diamond vacancy centers [4], spontaneous parametric down-conversion (SPDC) [5], and spontaneous four-wave mixing (SFWM) [6]. Among these processes, the SPDC and the SFWM processes create quantum-correlated photon pairs from one and two pump photons, respectively, and both processes require satisfying the energy conservation as well as phase matching [7]. Typically, the nonlinear coefficient of SPDC in second-order nonlinear crystals is larger than that of SFWM in amorphous single mode optical fibers as SFWM is a third-order nonlinear process. In the case of several hundred meters long single-mode fibers, however, the SFWM conversion efficiency from pump beam to photon pairs can be similar with that of the SPDC process in nonlinear crystals. In addition, the fiber based photon-pair sources are able to be directly coupled to fiber systems with negligible coupling loss, but waveguide-to-fiber coupling efficiency of a periodically poled SPDC crystal is reported about 50% [8]. The SFWM process has been studied intensively for the fiber-based photon generation [6, 9–20] for quantum information applications including quantum key distribution.

Photon-pair generation via SFWM is active near the zero group-velocity-dispersion (GVD) wavelength, λ_{ZGVD}, in the anomalous GVD regime [6, 9–15] or normal GVD regime [16–20]. In the normal GVD regime, the wavelength of the generated photon pairs is significantly detuned from the pump wavelength. In this case, Raman noise can be avoided, but the generated photon pair do not exhibit telecom-band wavelength together. On the other hand, in the anomalous GVD regime, the wavelength of the generated photon pair is slightly detuned from the pump in the telecom C-band and is strongly power dependent [16].

Since the wavelength of the generated pair is sensitive to the λ_{ZGVD} of the generation medium, several types of commercial fibers which have λ_{ZGVD} in the telecom C-band have been investigated as the telecom C-band pair sources. Even if commercial optical fibers have small tolerances in their physical properties, it is common to have sizeable λ_{ZGVD} variance along an optical fiber [21, 22]. Therefore, the precise measurement of the GVD spectrum is required, but it is often tricky with short length optical fibers. One way to overcome this problem is engineering the dispersion of a commercial fiber by heating and pulling the fiber, but this method is an ambitious research field [19, 20, 23]. On the other hand, if a slightly detuned pair can be generated in the normal GVD regime, the constraint for the λ_{ZGVD} of medium can be weakened, but it has not been reported to the best of our knowledge because phases are mis-matched in this regime due to the Kerr effects of the media.

© 2018 The Author(s). Published by IOP Publishing Ltd on behalf of Deutsche Physikalische Gesellschaft

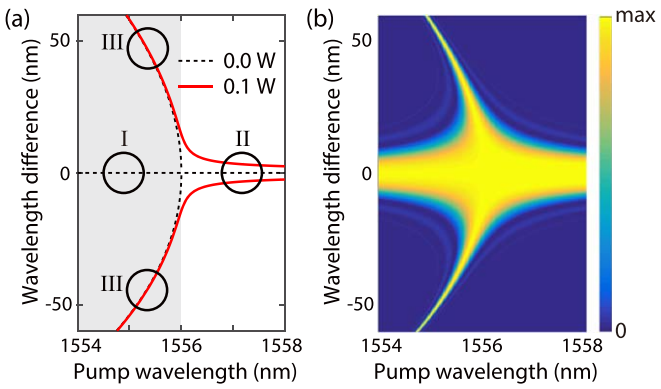

Figure 1. (a) Calculated phase matching curve against pump wavelength for a pump peak power of 0 W (black dashed line) and 0.1 W (red solid line) near $\lambda_{ZGVD} = 1555.98$ nm. (b) Normalized probability density spectrum of photon pair emission against pump wavelength for a pump peak power of 0.1 W with a 500 m DSF.

Here, we investigate the conditions for generating low-noise photon pairs in the telecom C-band that are slightly detuned from the pump wavelength in the normal GVD regime of dispersion shifted fiber (DSF) for the first time. Experimental conditions are carefully chosen to obtain high coincidence-to-accidental ratio (CAR) values by lowering temperature as well as pump power, reducing photon losses of the system, using a polarizer to block the cross-polarized Raman background photons, and selecting signal/idler photon filters at a small shift from the pump wavelength. A CAR value of about 260 was achieved, which is the highest value reported in DSF at liquid nitrogen temperatures. In addition, an excellent heralded anti-bunching property was achieved ($g_H^{(2)}(0) \sim 0.016$), indicating that this pair generation scheme is a potential low-noise photon-pair source or a heralded single-photon source. The results prove that the slightly detuned photon pair generation in the normal GVD regime in DSF can be effectively exploited as telecom-band quantum light sources for quantum information applications.

The photon-pair generation by SFWM needs to satisfy energy conservation and phase matching conditions as given by,

$$2\omega_p = \omega_s + \omega_i, \tag{1}$$

$$2k_p = k_s + k_i + 2\gamma P_p, \tag{2}$$

where ω_j (j = p, s, i) is the frequency of pump, signal, and idler photons ($\omega_s > \omega_i$), respectively, and $k_j \equiv n_j \omega_j / c$ (j = p, s, i) is the wave vector of the pump, signal, and idler photons in a DSF, respectively. n_j (j = p, s, i) is the frequency dependent refractive index of the medium and c is the speed of light in a vacuum. γ represents the nonlinear Kerr coefficient of the DSF and P_p is the pump peak power.

The λ_{ZGVD} of the DSF used in this study is 1555.98 nm. Using equations (1) and (2), the SFWM phase matching curve against the pump wavelength is calculated for the DSF with a peak pump power of 0 W (black dashed curves) and 0.1 W (red solid curves) as shown in figure 1(a). The y-axis represents the wavelength difference between the pump and the generated photons, and the photons with positive (negative) wavelength difference are idler (signal) photons. The regime with a shorter (longer) wavelength than $\lambda_{ZGVD} = 1555.98$ nm indicates the normal (anomalous) GVD regime and is represented as the gray (white) region.

When the pump peak power is 0 W, three solutions (I, II, and III) satisfying equations (1) and (2) exist as seen by the three black circles on the black dashed curves in figure 1(a). Solution I and II are the fundamental solutions with $k_p = k_s = k_i$, and solution III in the normal GVD regime is for signal/idler photons far from the pump wavelength ($k_p \neq k_s \neq k_i$ but $2k_p = k_s + k_i + 2\gamma P_p$). With a non-zero pump power, the photon pairs can be generated for the regime II and III (red curves in figure 1(a)) [6, 9–20], but the nonlinear Kerr effects, $2\gamma P_p$, in equation (2) cause difficulties in the generation of solution I for the normal GVD regime.

Figure 1(b) shows the normalized probability density spectrum of photon pair emission against the pump wavelength. Note that photon pairs close to the pump wavelength are created even in the normal GVD regime (solution I). The probability density spectrum of pair emission is based on the calculated joint spectral intensity through a 500 m DSF with a peak pump power of 0.1 W [15, 24]. The joint spectral intensity is proportional to $\mathrm{sinc}^2(\Delta kL/2)$, where L is the length of SFWM medium and $\Delta k = 2k_p - k_s - k_i - 2\gamma P_p$ is the phase mismatching. With an infinitely long DSF, the joint spectral intensity will be a delta function in the frequency domain and SFWM occurs only at the possible wavelengths from the phase matching curve as seen in figure 1(a). The phase matching can be, however, relaxed by using a finite length of SFWM medium and then photon pairs slightly detuned from the pump wavelength can be generated in the normal GVD regime as shown in figure 1(b).

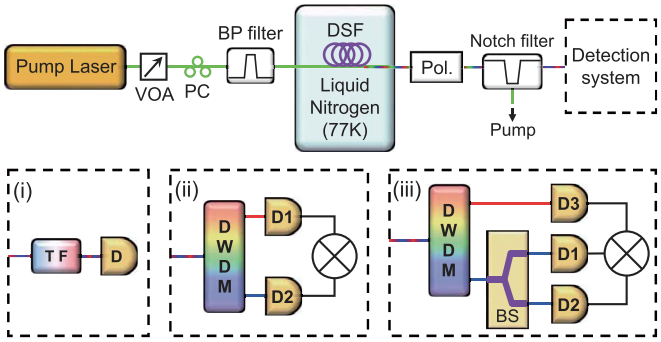

Figure 2. Experimental setup. A 10 ps pulse laser is the pump source with a repetition rate of 18 MHz at a center wavelength of 1552.52 nm, and the 500 m DSF is cooled to liquid nitrogen temperature. VOA: variable optical attenuator, PC: polarization controller, BP filter: band-pass filter, DSF: dispersion shifted fiber, Pol.: fiber polarizer, TF: tunable filter, DWDM: dense wavelength division multiplexing filter, BS: 50:50 fiber beam splitter, D: InGaAs APD single-photon detector. Inset: three different configurations of the detection system are used for (i) the single-photon spectrum, (ii) the CAR measurement, and (iii) the heralded second-order self-correlation measurement.

Figure 2 shows the experimental setup used in this study. The pump source is a mode-locked pulse laser with a pulse width of about 10 ps and a repetition rate of 18 MHz. Since C-band fiber optic components are commercially available, the pump and the filter wavelengths are anchored on the ITU grid. The pump wavelength selected in this study is 1552.52 nm (ITU-grid channel no. 31) which is about 3.5 nm away from λ_{ZGVD}. A set of 100 GHz dense wavelength division multiplexing (DWDM) filters with a full-width at half-maximum (FWHM) bandwidth of about 0.6 nm is used as a band-pass filter to remove amplified spontaneous emission noise from the pump laser. A variable optical attenuator adjusts the input pump power. The pump beam travels through the band-pass filter and enters a 500 m DSF which is cooled down to the temperature of liquid nitrogen to reduce spontaneous Raman scattering (spRS) [10–14]. In addition, a fiber polarizer is placed after the DSF to remove the cross-polarized Raman-scattered photons [9–11]. The measured values of λ_{ZGVD} and the dispersion slope of the used DSF fiber are 1555.98 nm and 69.7 s m^{-3}, respectively [25]. A set of notch filters with an FWHM bandwidth of 1.1 nm is used to attenuate the pump light by more than 120 dB. Furthermore, additional DWDM filters in the detection system suppress the pump light even more. The total suppression of the pump is more than 150 dB.

The experimental setup is identical for all experiments except the detection systems. Insets (i)–(iii) in figure 2 show the detection systems used for the following measurements: (i) the single-photon spectrum, (ii) the coincidence to accidental ratio (CAR), and (iii) the heralded second-order self-correlation. The 100 GHz DWDM filters separate signal and idler photons with an FWHM bandwidth of 0.6 nm. The total detection efficiency of setup (i) is about −20 dB including −7 dB InGaAs single-photon detector efficiency and that of setup (ii) and (iii) is −15.6 dB. The detection efficiency of idler photons in setup (iii) is about −19 dB including an additional 3 dB directional coupler. The gate width and the dead time of the single-photon detectors are 1 ns and 10 μs, respectively. The coincidence window of the time-correlated single photon counting (TCSPC) module in the experiments is about 500 ps.

The single-photon count spectrum (red squares in figure 3(a)) through a 500 m DSF is measured using the setup as shown in figure 2 with the detection system of inset (i) and a peak pump power of $P_p \sim 0.3$ W. The step size of the tunable filter is 25 GHz and the used notch filter has a flat transmittance reponse over the scanning range. Note that both the SFWM photons and spRS noise photons contribute to the single-photon count measurement (the red squares in figure 3(a)). Since the spRS spectrum does not depend on λ_{ZGVD}, the contribution of Raman noise photons to the single count spectrum can be estimated by the independent measurement of the spRS spectrum through a single-mode fiber (SMF, Corning (SMF-28)), as shown by the blue diamonds in figure 3(a). The different mode areas of the DSF and the SMF cause different photon noise rates, but the spectrums can be matched by applying a weight factor of about 1.5 to the SMF. Since the SMF has a λ_{ZGVD} at 1.3 μm, negligible photon-pair generation in this fiber is expected at 1552.52 nm.

As shown in figure 3(a), the SMF spectrum (blue diamonds) and DSF spectrum (red squares) show a meaningful difference between 1548 and 1557 nm. By subtracting these two spectra, the single-count spectrum due only to SFWM (black squares in figure 3(b)) is obtained. Since the photon generation rate by this process decreases rapidly and the photon noise rate due to spRS increases further away from the pump wavelength, the closer the signal and idler frequencies to the pump frequency, the larger the achievable signal-to-noise photon

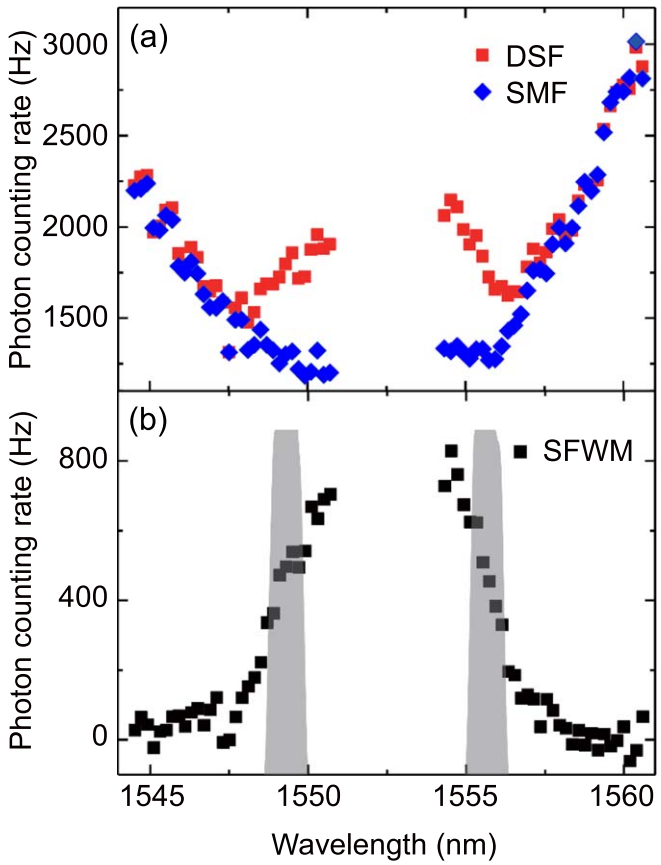

Figure 3. Single-photon spectrum measurements. (a) Measured single-photon spectra from a 500 m cooled DSF (red, square) and SMF (blue, diamond) and (b) extracted single-photon spectrum contributed by only the SFWM photons. The gray areas indicate the transmission spectra of filters which are represented by DWDM in insets of (ii) and (iii) of figure 2.

ratio. Considering the bandwidth of the notch filter and pump photon leakage through this filter as well as the DWDM, two commercially available DWDM channels of ITU-grid no. 35 (1549.32 nm) and 27 (1555.75 nm) are selected as the signal and idler photon filters, respectively. Their center frequency spacing from the pump is 400 GHz. The spectral shapes of the DWDM filters are shown in figure 3(b) as the gray areas.

The single count rate of each single-photon detector is measured for various pump peak powers using the detection system in inset (ii) of figure 2. The pair photons, spRS photons, and detector dark counts contribute to the count rate of each single-photon detector. The single count rate of each detector, C_A and C_B, can be written as [14],

$$C_A = \mu_P \alpha_s {P_p}^2 + \mu_{Rs} \alpha_s P_p + D_s, \tag{3}$$

$$C_B = \mu_P \alpha_i {P_p}^2 + \mu_{Ras} \alpha_i P_p + D_i, \tag{4}$$

where μ_j (j = P, Rs, Ras) is the generation rate of photon pairs, Stokes Raman photon, and anti-Stokes Raman photon, respectively. D_s (D_i) is the dark counts of the signal (idler) channel single-photon detector, P_p is the peak pump power, and $\alpha_s(\alpha_i)$ is the product of the total transmittance and the quantum efficiency of the detector for each channel.

The square markers in figures 4(a) and (b) are the measured signal and idler count rates against the peak pump power, respectively. The theoretical fit obtained using equations (3) and (4) are shown as black solid curves superimposed on the experimental data. The dashed and dotted curves represent the quadratic and linear contributions of the fitting functions corresponding to the photon-pair generation and the spRS rates, respectively. The dark count rates in this experiment are negligible (~50 Hz).

The single count rate in figures 4(a) and (b) has a maximum count value of 10.8 kHz, which is limited by the detector performance and not the photon-pair source. The InGaAs single-photon detectors used in this experiment are operated with 10 μs dead time to avoid the after-pulsing effects, and the pair generation rate is reduced to prevent the saturation effects of the detectors. In addition, the −15.6 dB total detection efficiency needs to be improved for fast measurements. Much higher single and coincidence count rates are expected if fast

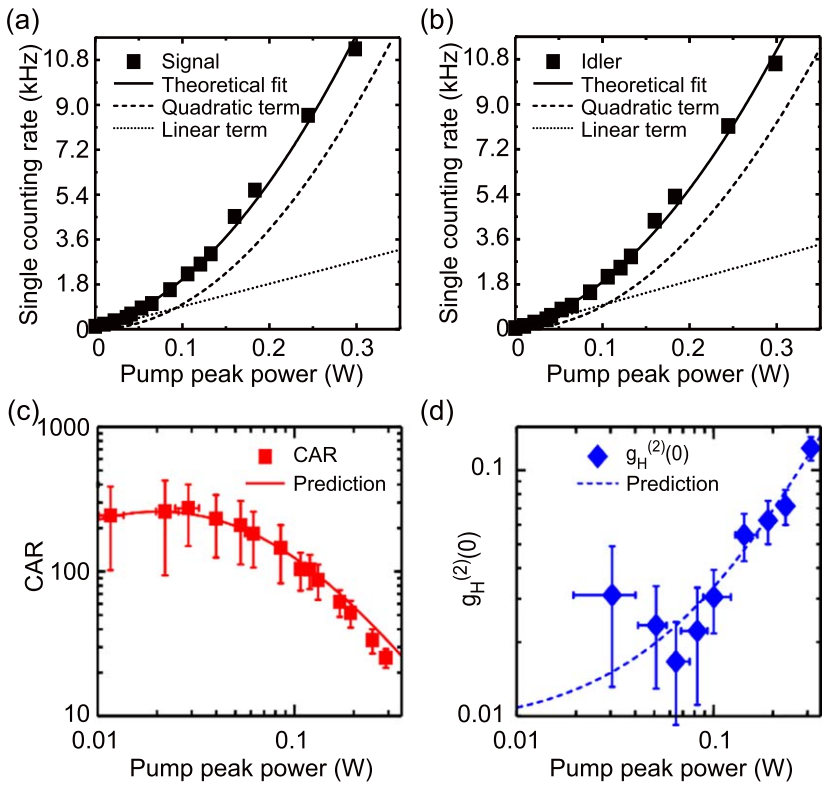

Figure 4. Measured (a) single counts of the signal, (b) single counts of idler, (c) CAR, and (d) heralded second-order self-correlation against the pump peak power. The solid lines in (a) and (b) are quadratic fittings of measured data. Dashed and dotted lines represent quadratic and linear contributions of the fitting functions, respectively. The solid red curve in (c) and the dashed blue curve in (d) are the expected values of CAR and the heralded second-order self-correlation that are extracted from the single count measurements in (a) and (b). All measurements were performed by using the DWDM filters represented as the gray areas in the figure 3(b).

and efficient single-photon detectors are used such as superconducting nanowire detectors [12, 14] or up-conversion detectors [26]. In addition, the active spatial multiplexing method of multiple photon-pair sources can increase the pair generation rate while keeping low CAR [27].

Figure 4(c) shows the result of the CAR measurements against the pump power, where a maximum CAR value of 260 is obtained. The red squares mean the measured CAR values, the horizontal error bar is the pump power fluctuation during measurement, and the vertical error bar represents the shot noise assuming a Poisson distribution of photons. Under our experimental conditions, the accumulation times of each data point in figures 4(c) and (d) differ from each other for reducing the total measurement time. Therefore, the size of the error bars fluctuates due to the uneven accumulation time, but the power dependence of the measured CAR values is not affected and is in close agreement with the predicted CAR values (red solid curve in figure 4(c)).

The coincidence count rate, C_{AB}, is given by $\mu_P\alpha_s\alpha_i P_p^2 + C_A C_B$, where $C_A C_B$ is the accidental coincident rate including pair–pair, Raman–Raman, and pair–Raman coincidences. This relation explains why the CAR value is about 25 for a 0.3 W pump peak power in figure 4(c), even though the measured spRS single count rate ($N_{spRS} \sim 1300$ Hz) in figure 3(a) is higher than the measured SFWM single count rate ($N_{SFWM} \sim 450$ Hz) in figure 3(b). The pair generation rate per pulse is given by $\mu_P P_p^2/R = (N_{SFWM}/\eta)/R$, where η represents the total detection efficiency and R is the pump repetition rate. Similarly, the Raman generation rate is $\mu_{Rs}P_p/R = (N_{spRS}/\eta)/R$. From the above coincidence count rate C_{AB}, the true coincidence count rate is $\{(N_{SFWM}/\eta)/R\} \times \alpha_s\alpha_i R$ and the accidental coincidence count rates by multiple pairs, Raman photons, and the combination of them are $\{(N_{SFWM}/\eta)/R + (N_{spRS}/\eta)/R\}^2 \times \alpha_s\alpha_i R$. The accidental due to the dark counts of two detectors is neglected. The CAR is given by $\{(N_{SFWM}/\eta)/R\}/\{(N_{SFWM}/\eta)/R + (N_{spRS}/\eta)/R\}^2$ and the estimated CAR value is about 26 using the parameters of $R = 18 \times 10^6$ (MHz) and $\eta = -20$ dB for the setup (i) in figure 2, showing excellent agreement with the experimental result of 25 in figure 4(c).

The highest CAR value 260 at a peak pump power of 20 mW is smaller than that of the Raman-free pair photon generation processes. However, the CAR value of 260 is about twice as large the previously reported value for DSF at the same temperature of 77 K in the anomalous GVD regime [10–12]. This result implies that a CAR of 3000 is expected if a DSF is cooled down to the temperature of liquid helium at about 4.2 K [12].

To characterize the heralded single-photon property of the generated photons, the conditional Hanbury-Brown and Twiss (HBT) experiment is performed to measure the heralded second-order self-correlation, $g_H^{(2)}(0)$.

The detection system of the conditional HBT experiment is shown in inset (iii) of figure 2. Signal photons are used as the heralding photons (D3), and the self-correlation of the idler photons is measured under the heralded condition. The three-fold coincidence of D1, D2, and D3 is counted using a TCSPC module with a coincidence window of about 500 ps. Using the pulsed pump, $g_{\mathrm{H}}^{(2)}(0)$ is given by [27, 28],

$$g_{\mathrm{H}}{}^{(2)}(0) = \frac{C_{\mathrm{ABH}}(0)\,C_{\mathrm{H}}}{C_{\mathrm{AH}}(0)\,C_{\mathrm{BH}}(0)}, \tag{5}$$

where C_{ABH} is the three-fold coincidence counts of D1, D2, and D3, C_{AH} (C_{BH}) is the heralded coincidence counts of D3 and D1 (D3 and D2), and C_{H} is the heralding single counts of D3.

Figure 4(d) shows the measured $g_{\mathrm{H}}^{(2)}(0)$ values (blue diamond dots) against the peak pump power. The horizontal error bar represents the pump power fluctuation while the vertical error bar represents the shot noise. The blue dashed curve represents the $g_{\mathrm{H}}^{(2)}(0)$ values using equation (5) and the single count measurements in figures 4(a) and (b). As the peak pump power decreases, $g_{\mathrm{H}}^{(2)}(0)$ is reduced and the measured minimum value was 0.0167 ± 0.0075. Therefore, the SFWM source used in this experiment can create photon pairs with strong temporal correlation and can be an excellent heralded single-photon source with a high signal-to-noise ratio.

In summary, photon pairs that are slightly detuned from the pump wavelength in the normal GVD regime are observed in the telecom C-band through a DSF for the first time. The photon noise due to spRS is reduced by lowering the temperature to 77 K, using a polarizer, and employing a low Raman scattering wavelength. A high CAR value of 260 was obtained and this value is the maximum value reported in DSF at liquid nitrogen temperature. The excellent anti-bunching property of the heralded single photons is confirmed using the conditional HBT experiment with a minimum $g_{\mathrm{H}}^{(2)}(0)$ value of 0.0167 ± 0.0075. The results show that the slightly detuned photon pair generated in the normal GVD regime has good temporal correlation properties that are comparable to photon pairs generated in the anomalous GVD regime. The generation scheme used in this paper shows potential for application as an efficient photon-pair source or pure heralded single photon generation source in the telecom C-band. Even though pair generation through a DSF is limited by spRS noise, our results show that the DSF system in the normal GVD regime can be used as a practical photon-pair source that would have a direct positive impact on quantum information processing.

These relaxed phase matching conditions extend the terms of photon pair generation. We believe that the relaxed phase matching conditions will occur not only in DSF but also in all the SFWM media such as photonic crystal fiber, highly nonlinear fiber, and silicon waveguide. Therefore, the relaxed phase matching scheme will be useful for the development of efficient photon-pair sources along with the techniques of engineering the chromatic dispersion of optical waveguides.

Acknowledgments

This work was supported by the KIST Open Research Program (2E27230-17-P005) and the National Research Foundation of Korea (2016R1A4A1008978, 2016K1A3A1A12953720).

References

[1] Lounis B and Moerner W E 2000 Single photons on demand from a single molecule at room temperature *Nature* **407** 491
[2] Kuhn A, Hennrich M and Rempe G 2002 Deterministic single-photon source for distributed quantum networking *Phys. Rev. Lett.* **89** 067901
[3] Gazzano O, Michaelis de Vasconcellos S, Arnold C, Nowak A, Galopin E, Sagnes I, Lanco L, Lemaitre A and Senellart P 2013 Bright solid-state sources of indistinguishable single photons *Nat. Commun.* **4** 1425
[4] Kurtsiefer C, Mayer S, Zarda P and Weinfurter H 2000 Stable solid-state source of single photons *Phys. Rev. Lett.* **85** 290
[5] Shih Y H and Alley C O 1988 New type of Einstein–Podolsky–Rosen–Bohm experiment using pairs of light quanta produced by optical parametric down conversion *Phys. Rev. Lett.* **61** 2921
[6] Fiorentino M, Voss P L, Sharping J E and Kumar P 2002 All-fiber photon-pair source for quantum communications *IEEE Photonics Technol. Lett.* **14** 983–5
[7] Bienfang J C, Fan J, Migdall A and Polyakov S V 2013 *Sigle-Photon Generation and Detection* ed A Migdall *et al* (Amsterdam: Elsevier)
[8] Zhong T, Franco N C, Roberts T D and Battle P 2009 High performance photon-pair source based on a fiber-coupled periodically poled $KTiOPO_4$ waveguide *Opt. Express* **17** 12019–30
[9] Li X, Chen J, Voss P L, Sharping J E and Kumar P 2004 All-fiber photon-pair source for quantum communications: improved generation of correlated photons *Opt. Express* **12** 3737–44
[10] Takesue H and Inoue K 2005 1.5 μm band quantum-correlated photon pair generation in dispersion-shifted fiber: suppression of noise photons by cooling fiber *Opt. Express* **13** 7832–9
[11] Lee K F, Chen J, Liang C, Li X, Voss P L and Kumar P 2006 Generation of high-purity telecom-band entangled photon pairs in dispersion-shifted fiber *Opt. Lett.* **31** 1905–7
[12] Dyer S D, Stevens B J, Baek B and Nam S W 2008 High-efficiency, ultra low-noise all-fiber photon-pair source *Opt. Express* **16** 9966–77
[13] Zhou Q, Zhang W, Cheng J, Huang Y and Peng J 2011 Properties of optical fiber based synchronous heralded single photon sources at 1.5 μm *Phys. Lett.* A **375** 2274–7

[14] Dong S, Zhou Q, Zhang W, He Y, Zhang W, You L, Huang Y and Peng J 2014 Energy–time entanglement generation in optical fibers under CW pumping *Opt. Express* **22** 359–68
[15] Li X, Ma X, Ou Z Y, Yang L, Cui L and Yu D 2008 Spectral study of photon pairs generated in dispersion shifted fiber with a pulsed pump *Opt. Express* **16** 32–44
[16] Rarity J G, Fulconis J, Duligall J, Wadsworth W J and Russell P S J 2005 Photonic crystal fiber source of correlated photon pairs *Opt. Express* **13** 534–44
[17] Fulconis J, Alibart O, Wadsworth W J, Russell P S J and Rarity J G 2005 High brightness single mode source of correlated photon pairs using a photonic crystal fiber *Opt. Express* **13** 7572–82
[18] Söller C, Cohen O, Smith B J, Walmsley I A and Silberhorn C 2011 High-performance single-photon generation with commercial-grade optical fiber *Phys. Rev.* A **83** 031806 (R)
[19] Cui L, Li X, Guo C, Li Y H, Wang L J and Fang W 2013 Generation of correlated photon pairs in micro/nano-fibers *Opt. Lett.* **38** 5063–6
[20] Kim J-H, Ihn Y S, Shin H and Kim Y-H 2017 Generation of near-infrared correlated photon pairs in a long optical nano-fibers *Frontiers in Optics* **2017** JW3A.21
[21] Schlager J B, Mechels S E and Franzen D L 1996 Zero-dispersion wavelength uniformity and four-wave mixing in optical fiber Conf. Proc. LEOS'96 9th Annual Meeting IEEE Lasers and Electro-Optics Society *(Boston, MA, USA, 18–21 November 1996)* (Piscataway, NJ: IEEE) pp 166–7
[22] Francis-Jones R J A and Mosley P J 2016 Characterisation of longitudinal variation in photonic crystal fibre *Opt. Express* **24** 273756
[23] Ortiz-Ricardo E, Bertoni-Ocampo C, Ibarra-Borja Z, Ramirez-Alarcon R, Cruz-Delgado D, Cruz-Ramirez H, Garay-Palmett K and U'ren A B 2017 Spectral tunability of two-photon states generated by spontaneous four-wave mixing: fibre tapering, temperature variation and longtudinal stress *Quantum Sci. Technol.* **2** 034015
[24] Garay-Palmett K, McGuinness H J, Cohen O, Lundeen J S, Rangel-Rojo R, U'Ren A B, Raymer M G, McKinstrie C J, Radic S and Walmsley I A 2007 Photon pair-state preparation with tailored spectral properties by spontaneous four-wave mixing in photonic-crystal fiber *Opt. Express* **15** 14870–86
[25] Jung S J, Lee J Y and Kim D Y 2006 Novel phase-matching condition for a four wave mixing experiment in an optical fiber *Opt. Express* **14** 35–43
[26] Thew R T *et al* 2006 Low jitter up-conversion detectors for telecom wavelength GHz QKD *New J. Phys.* **8** 32
[27] Collins M J *et al* 2013 Integrated spatial multiplexing of heralded single-photon sources *Nat. Commun.* **4** 2582
[28] Beck M 2007 Comparing measurements of $g^{(2)}(0)$ performed with different coincidence detection techniques *J. Opt. Soc. Am.* B **24** 2972–8